

# Static active-matrix OLED display without pixel refresh enabled by amorphous-silicon non-volatile memory

Yifei Huang

Bahman Hekmatshoar (SID Student Member)

Sigurd Wagner

James C. Sturm

**Abstract** — An active-matrix organic light-emitting-diode (AMOLED) display which does not require pixel refresh is demonstrated. This was achieved by replacing the thin-film transistor (TFT) that drives the OLED with a non-volatile memory TFT, in a 2-transistor pixel circuit. The threshold voltage of the non-volatile-memory TFT can be changed by applying programming voltage pulses to the gate electrode. This approach eliminates the need for storage capacitors, increases the pixel fill factor, and potentially reduces power consumption. Each pixel can be individually programmed or erased using a standard active-matrix addressing scheme. The programmed image is stored in the display even if power is turned off.

**Keywords** — Amorphous silicon, thin-film transistor, non-volatile memory, AMOLED display.

DOI # 10.1889/JSID18.11.879

## 1 Introduction

There is growing interest in the development of novel AMOLED pixel circuitry to reduce power consumption and improve fill factor. Traditionally, AMOLED displays require periodic pixel refreshes, which consume power to recharge the storage capacitor even if the image is not changing. The storage capacitor also reduces pixel fill factor. In this work, we take advantage of the recent developments in a-Si non-volatile memory,<sup>1–3</sup> and demonstrate an AMOLED display that stores and displays images without pixel refreshes.

## 2 Background

The conventional AMOLED pixel [Fig. 1(a)] has two TFTs, a storage capacitor, and an OLED. During display operation, the select line is pulled high to allow the voltage on the data line to propagate through the switching TFT to the storage node, charging the storage capacitor and the gate electrode of the driver TFT. This sets the current through the driver TFT and OLED, and consequently the brightness of the pixel. The storage capacitor is necessary to hold the voltage on the gate of the driver TFT between pixel refreshes, but it also reduces the active light-emitting area of the pixel and thus the fill factor of the pixel. Furthermore, because the charge on the storage capacitor leaks through the switching TFT over time, the pixel must be refreshed (or recharged) periodically. In low-frame-rate applications, these excess refresh cycles are required to simply maintain the image, not to introduce new image data into the pixels.

We propose a new pixel structure [Fig. 1(b)] to address these two issues by integrating an a-Si memory TFT as the

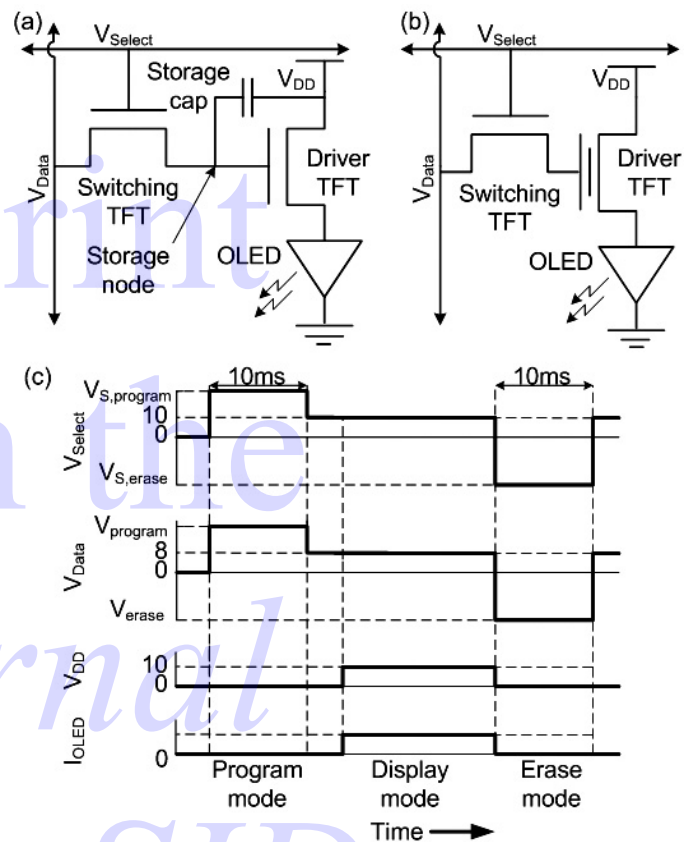


**FIGURE 1** — (a) Conventional 2-TFT AMOLED pixel with the storage capacitor used to hold the voltage on the gate electrode of the driver TFT between pixel refreshes. (b) A 2-TFT AMOLED pixel with integrated memory device. (c) Timing diagram showing the modes of operation in the new pixel in (b).

driver TFT. These memory TFTs will be referred to as SiN<sub>x</sub> trap TFTs (ST-TFTs) from here on. The ST-TFT has excellent memory characteristics, including a room-temperature

Received 06/17/10; accepted 08/23/10.

The authors are with the Princeton Institute for the Science and Technology of Materials (PRISM), Department of Electrical Engineering, Princeton University, Princeton, NJ 08544, USA; telephone 646/240-5618, e-mail: yhtwo@princeton.edu.

© Copyright 2010 Society for Information Display 1071-0922/10/1811-0879\$1.00.

retention time greater than 10 years.<sup>3</sup> It uses a high-defect-density interface, embedded in the gate dielectric layer, to trap charges injected by short duration (typically 10 msec) voltage pulses applied to the gate. By varying the magnitude of the programming pulse, we can control the threshold voltage ( $V_T$ ) of a ST-TFT. In the new pixel circuit with the ST-TFT driver, the OLED brightness is *not* controlled by varying the  $V_{DATA}$  applied to the gate of the driver ST-TFT through the switching TFT, as in a conventional AMOLED pixel. Instead, a constant  $V_{DATA}$  is applied to the gate of the driver ST-TFT. The current through the driver ST-TFT and the OLED brightness is controlled by changing the  $V_T$  of the ST-TFT through programming. If low brightness is desired, the ST-TFT is set to a high  $V_T$  by programming with a large positive gate pulse. If high brightness is desired, the ST-TFT is set to a low  $V_T$  by programming with a small positive gate pulse, or not programming at all and leaving it with the initial  $V_T$ .

A given pixel in a display is programmed by applying a high magnitude (*e.g.*, 35 V) and short duration (*e.g.*, 10 msec) voltage pulse to the corresponding data line [program mode in Fig. 1(c)]. The same voltage pulse (plus  $\sim 2$  V to account for threshold voltage of the switching TFT) is applied to the corresponding select line to allow the  $V_{DATA}$  pulse to propagate to the gate of the desired driver ST-TFT. All other select lines are held at ground to prevent the  $V_{DATA}$  pulse from programming other undesired pixels.  $V_{DD}$  is held at ground during programming to ensure both the source and the drain of the ST-TFT are at 0 V. This process is repeated until all pixels in the display have been programmed to their respective brightness values.

After programming, the display is activated by setting  $V_{DD}$  to 10 V [display mode in Fig. 1(c)],  $V_{DATA}$  to 8 V on all the data lines, and  $V_{SELECT}$  to 10 V on all the select lines. The OLED current and therefore brightness of any given pixel is determined by the programmed  $V_T$  of the driver ST-TFT. High  $V_T$  translates into a small OLED current and a dim pixel, and a low  $V_T$  translates into large OLED current and a bright pixel. It is important to note that both  $V_{DATA}$  and  $V_{SELECT}$  are DC voltages in the display mode because a pixel refresh is not necessary to maintain a static image. The image information remains stored in the ST-TFT threshold voltage even if the power is turned off.

To change the programmed image, the pixels are first erased and then programmed again. Erase mode, shown in Fig. 1(c), is identical to the program operation. The only difference is that the applied voltage pulse has a large negative magnitude, instead of a positive one. This negative voltage forces the trapped electrons in the ST-TFT to tunnel back out, causing  $V_T$  to shift towards its original unprogrammed value. Note that to erase a single pixel in the active matrix (instead of an entire column), all other select lines would have to be held at  $-30$  V to prevent the erase pulse from propagating to the undesired pixel drivers.

### 3 Fabrication

The a-Si ST-TFT and the AMOLED backplane were fabricated using a process that is identical to that of the conventional bottom-gate a-Si TFT, except for one key step – the formation of the  $\text{SiN}_x$  traps. After the control gate dielectric in the ST-TFT is deposited using plasma-enhanced chemical vapor deposition (PECVD), reactive ion etch (RIE) is used to create etch damage on the  $\text{SiN}_x$  surface. The etch damage results in midgap trap states, which are the workhorse of the ST-TFT memory. The traps are then encapsulated with the tunnel  $\text{SiN}_x$ , and the process follows that of a conventional bottom gate a-Si TFT from this point forward. More details of the a-Si ST-TFT and AMOLED backplane fabrication process are described in Refs. 3–5. After the completion of the backplane, which consists of the TFTs and the interconnect lines, the sample is encapsulated with a 300-nm-thick  $\text{SiN}_x$  layer deposited via PECVD. This layer serves as insulation between the backplane and the OLEDs. Via holes are etched into the passivation  $\text{SiN}_x$  using RIE to allow contact between the source of the driver TFT and indium–tin–oxide (ITO), which is the anode of the OLEDs. A 250-nm-thick ITO layer was deposited via RF sputtering with a gas mixture of  $\text{Ar}/\text{O}_2$  (99%/1%) at room temperature. The ITO layer is patterned via wet etching with aqua regia ( $\text{HNO}_3/\text{HCl}/\text{H}_2\text{O}$  1:5:6). A 1.4- $\mu\text{m}$ -thick photo-patternable planarization resist is spin-coated over the entire sample, and patterned to reveal the flat portions of the ITO anodes. The planarization resist is reflowed at 180°C to provide smooth edges that cover the rough features of the circuits and interconnect below. This improves the yield of the OLEDs by reducing the chance of short-circuit faults. The sample is exposed to UV-ozone for about 5 minutes, to increase the surface work function of the ITO anode and improve hole-injection efficiency.<sup>6</sup> An organic multilayer of *N,N'*-diphenyl-*N,N'*-bis(3-methylphenyl)-1,1'-biphenyl-4,4'-diamine (TPD)/aluminum tris(8-hydroxyquinoline) (Alq3) was deposited via thermal evaporation to form green luminescent diodes.<sup>7</sup> The thicknesses of both layers were  $\sim 30$  nm. A bilayer of Mg/Ag (20 nm/100 nm) is evaporated via thermal evaporation to form the cathode of the OLEDs.

The cross section of the completed pixel is shown in Fig. 2. The pixel area is 0.2 mm<sup>2</sup>. The switching TFT is 5  $\mu\text{m}$ /5  $\mu\text{m}$  and the driver TFT is 150  $\mu\text{m}$ /15  $\mu\text{m}$ . With a design rule of 10  $\mu\text{m}$ , the fill factor is 81%, a 15% improvement over the 66% fill factor of a conventional pixel fabricated with the same design rule and TFT dimensions.

### 4 Results and discussion

The pixel current–voltage characteristics were first measured prior to OLED integration by applying a  $V_{DD}$  of 10 V, a  $V_{SELECT}$  of 10 V, grounding the source of the driver ST-TFT (OLED anode) and sweeping  $V_{DATA}$  from 0 to 8 V in 50-mV increments.  $V_{DATA}$  should be fully transferred to the gate voltage of the ST-TFT for slow scans, and with initial

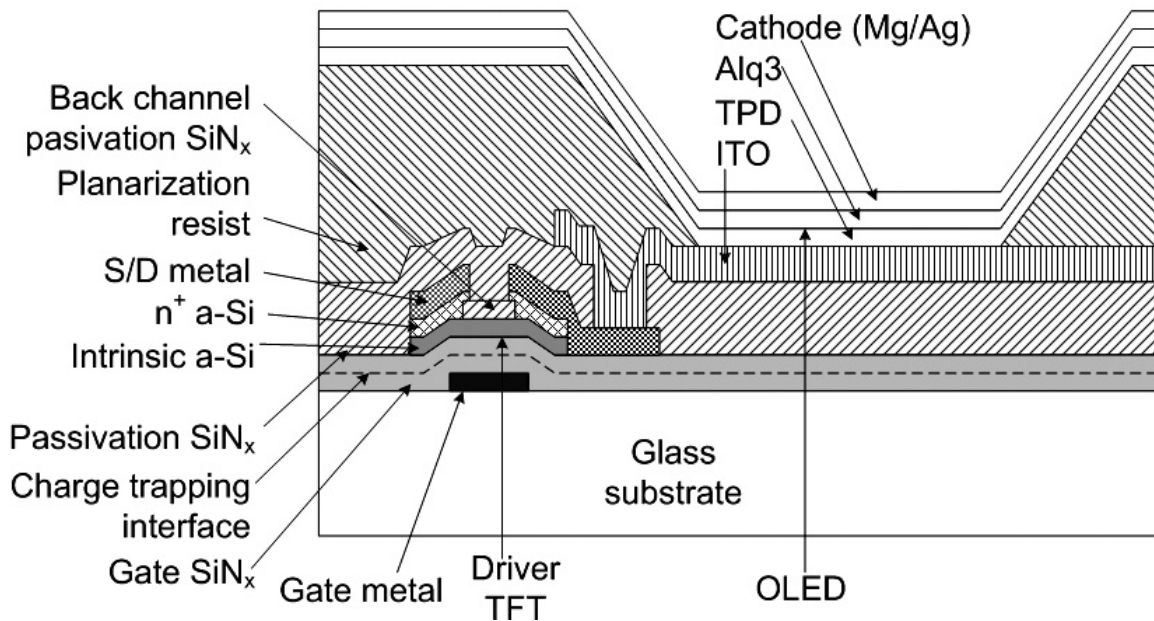


FIGURE 2 — Cross-sectional structure of AMOLED pixel with integrated a-Si non-volatile memory TFT.

TFT threshold voltage of  $\sim 1.5$  V, the TFTs are in saturation mode. The curve marked “before program” in Fig. 3 is the pixel current *vs.*  $V_{DATA}$  characteristic of the as-fabricated pixel, and the one marked “after program at 35 V” is the pixel characteristic after a 10 msec 35-V programming pulse (with  $V_{SELECT} = 37$  V) has been applied to the data lines with  $V_{DD}$  grounded. A clear  $V_T$  shift of  $\sim 2$  V is observed. Consequently, under the same bias conditions, the programmed pixel would provide less drive current than the unprogrammed pixel, resulting in a dimmer OLED. The curve marked as “after erase” is the pixel characteristic after

the programmed pixel has been erased with a 10-msec  $-28.5$ -V voltage pulse on  $V_{DATA}$  ( $V_{SELECT} = -26.5$ ). It can be seen that the programming-induced  $V_T$  shift can be reversed *via* the erase operation and the pixel characteristics returned that of the unprogrammed state. More detailed characterization of the ST-TFT can be found elsewhere.<sup>3</sup>

Figure 4 shows the pixel brightness in an isolated test pixel as a function of programming voltage, after OLED integration with the cathode grounded. The pixel brightness is measured with fixed  $V_{DATA} = 8$  V,  $V_{DD} = 10$  V, and  $V_{SELECT} = 10$  V. The measured pixel brightness decreases with increasing magnitude of the programming voltage pulse, with the pixel turned completely off for a programming voltage

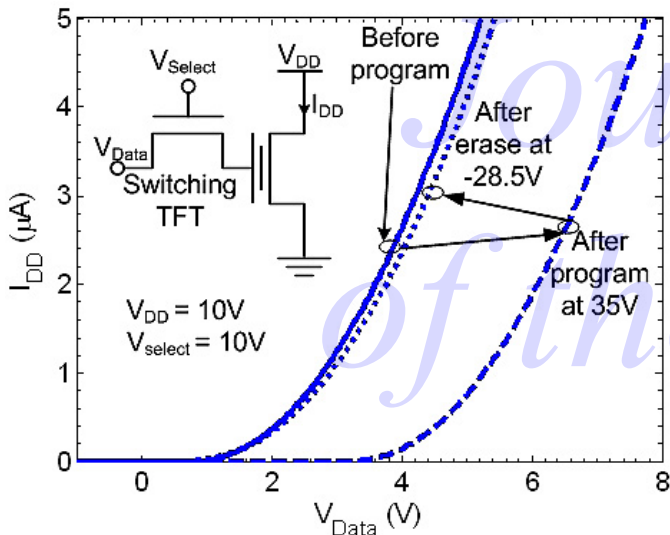


FIGURE 3 — Single-pixel current *vs.*  $V_{DATA}$  characteristics before OLED integration. The aspect ratios of the driver TFT and switching TFT are 10 and 1, respectively. The curves are shown for pixel before programming, after programming at 35 V ( $V_{SELECT} = 37$  V) for 10 msec, and after erasing at  $-28.5$  V ( $V_{SELECT} = -26.5$  V) for 10 msec.

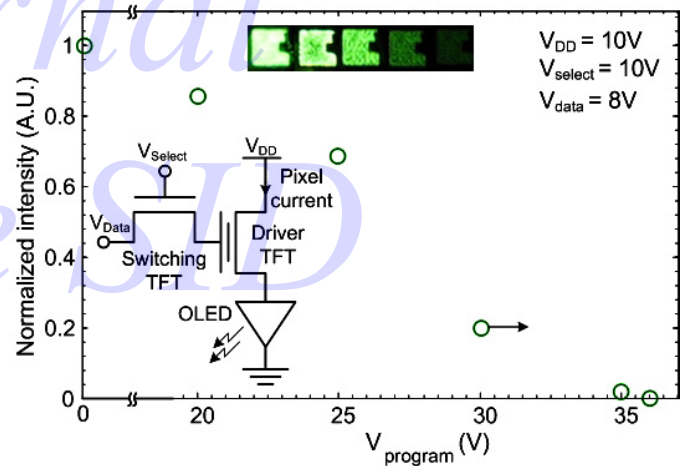
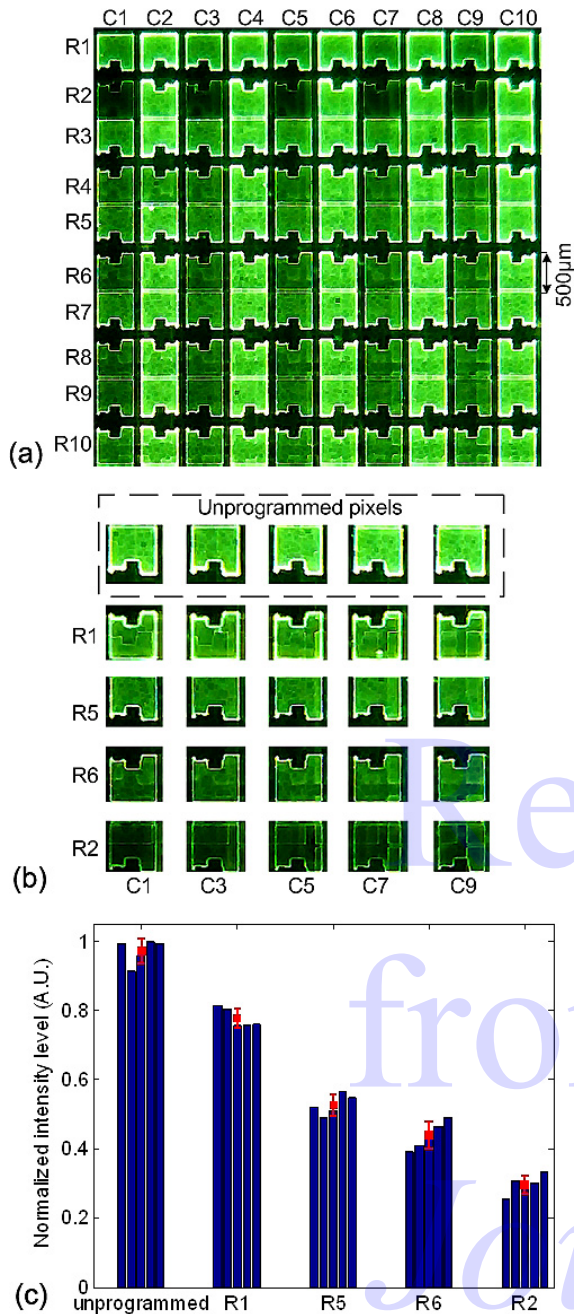


FIGURE 4 — Single pixel brightness as a function of programming voltage, after OLED integration. The inset shows photographs of five individual pixels, corresponding in order to the programming conditions of 0, 20, 25, 30, and 35 V. The aspect ratios of the driver TFT and switching TFT are 10 and 1, respectively.



**FIGURE 5** — (a) Photograph of an integrated  $10 \times 10$  AMOLED display. The even columns (C2, C4, C6, C8, and C10) have not been programmed. The odd columns (C1, C3, C5, C7, and C9) are tied together and have been programmed to four different intensity levels, with programming voltages of 20 V (R1, R3 and R10), 24 V (R5 and R7), 28 V (R4, R6, R8 and R9), and 32 V (R2). (b) Representative pixels from each of the four different programmed intensity levels, along with the unprogrammed pixels (from the even columns), are reproduced to for better viewing comparison. (c) Measured brightness statistics of the pixels from the array.

of 37 V. The trend is in agreement with the expectation that as the threshold voltage shift of the driver ST-TFT increases with increasing programming voltages.

Figure 5(a) shows the photograph of an integrated  $10 \times 10$  AMOLED display. All the even data lines (columns) are tied together, and all the odd data lines are tied together for simplified testing. The select lines (rows) can be accessed

individually. The odd columns were programmed by applying programming voltage pulses to the odd data lines, and no programming was done on the even columns. Programming was performed one row at a time, by activating the row select lines with the appropriate voltage pulse. Because the odd column data lines were tied together, all the odd-column pixels in a given row are programmed to the same intensity. The rows were programmed to four different intensity levels with programming voltages of 20, 25, 27, and 30 V. After programming, the display was driven with constant DC voltages of  $V_{DD} = 10$  V,  $V_{SELECT} = 10$  V, and  $V_{DATA} = 8$  V. Representative pixels of each intensity level, along with unprogrammed pixels (from even rows), are reproduced in Fig. 5(b) for better brightness comparison. R1, R5, R6, and R2 are programmed with 20, 24, 28, and 32 V, respectively. As the programming voltage is increased, raising the ST-TFT threshold, the brightness of the pixel decreases as expected. Figure 5(c) shows the brightness-level statistics of pixels from an integrated AMOLED display. Pixels that have been programmed to the same brightness exhibit a standard deviation in brightness of  $\sim 4\%$ , demonstrating good uniformity and control in setting the pixel brightness.

## 5 Conclusion

We have successfully demonstrated a new approach for the control of pixel brightness in static and low-refresh-rate applications, by integrating a-Si non-volatile-memory TFTs into the pixel circuit. Because the display does not need storage capacitors, it achieves a better fill factor and does not need power-consuming refresh cycles. The brightness is controlled by adjusting the threshold voltage of the OLED driver TFT.

## References

1. Y. Kuo and H. Nominanda, "Nonvolatile hydrogenated-amorphous-silicon thin-film-transistor memory devices," *Appl. Phys. Lett.* **89**, 173503-6 (October 2006).
2. Y. Huang *et al.*, "Amorphous silicon floating gate transistor," *Proc. of 67th Annual Device Research Conference, Conference Digest*, 135-136 (June 2009).
3. Y. Huang *et al.*, "High retention-time nonvolatile amorphous silicon TFT memory for static active matrix OLED display without pixel refresh," *Proc. of 68th Annual Device Research Conference, Conference Digest*, 179-180 (June 2010).
4. T. Tsujimura *et al.*, "A 20-in. OLED display driven by Super-a-Si Technology," *SID Symposium Digest* **34**, No. 6 (2003).
5. K. R. Sarma *et al.*, "Active matrix OLED using  $150^\circ\text{C}$  a-Si TFT back-plane built on flexible plastic substrate," *SPIE Proc.* **5080**, 180-191 (April 2003).
6. K. Sugiyama *et al.*, "Dependence of indium-tin-oxide work function on surface cleaning method as studied by ultraviolet and x-ray photoemission spectroscopies," *J. Appl. Phys.* **87**, 295 (2000).
7. H. Mu *et al.*, "Dependence of film morphology on deposition rate in ITO/TPD/Alq<sub>3</sub>/Al organic luminescent diodes," *Solid-State Electron.* **48**, Issues 10-11, 2085-2088 (Nov. 2004).



**Yifei Huang** received his B.S.E. degree from the Electrical-Engineering Department at Cooper Union, New York, NY, in 2006, and M.A. degree from Princeton University, Princeton, NJ, in 2008, where he is currently working towards his Ph.D. degree in electrical engineering. His research focus is on amorphous-silicon thin-film devices.



**Bahman Hekmatshoar** received his B.Sc. and M.Sc. degrees in electrical engineering from the University of Tehran, Tehran, Iran, in 2002 and 2004, respectively. He is currently working toward the Ph.D. degree in the Electrical Engineering Department at Princeton University, Princeton, NJ. His research focus is on thin-film transistor-backplanes on flexible plastic substrates.



**Sigurd Wagner** received his Ph.D. degree from the University of Vienna, Vienna, Austria, in 1968. He was a Postdoctoral Fellow at Ohio State University, Columbus, OH, a Member of the Technical Staff of the Bell Telephone Laboratories, Chief of the Photovoltaic Research Branch of the Solar Energy Research Institute, and, since 1980, Professor of Electrical Engineering at Princeton University, Princeton, NJ. He is developing technology for flexible large-area electronics, electrotextiles, and elastic electronic skin. His research is focused on: (1) flexible backplanes using amorphous, nanocrystalline, and microcrystalline silicon on plastic and steel foil; (2) the interdependence of electrical and mechanical properties in film-on-foil electronics when rolled, conformally shaped, or stretched; and (3) functional cells for large-area electronics and microfluidics, including displays, multifunctional materials, electrotexiles, and sensor skin.



**James C. Sturm** received his B.S.E. degree in electrical engineering and engineering physics from Princeton University, Princeton, NJ, and M.S.E.E and Ph.D. degrees in electrical engineering from Stanford University, Stanford, CA, in 1981 and 1985, respectively. He joined the faculty of Princeton University in 1986, where he is currently a Professor of Electrical Engineering and the PRISM Director. His previous experience includes his work at Intel Corp. as microprocessor design engineer as well as Siemens, Munich, Germany. He has worked in the fields of silicon-based heterojunctions, three-dimensional integration, silicon-on-insulator, optical interconnects, TFT's, and organic light-emitting diodes. His current research interests include silicon-germanium-carbon and related heterojunctions on silicon, SOI, and 3-D integration, large-area electronics, flat-panel displays, organic semiconductors, and the nanotechnology-biology interface. Prof. Sturm is a Fellow of IEEE and a member of the American Physical Society, and the Materials Research Society. Formerly, he was a National Science Foundation Presidential Young Investigator. In 1994 and 1995, he was a von Humboldt Fellow at the Institut Für Halbleitertechnik at the University of Stuttgart, Germany. He has won ten awards for teaching excellence from both Princeton University and the Keck Foundation, and in 2004 received the President's Distinguished Teaching Award at Princeton. In 1996 and 1997 he was the technical program chair and general chair of the IEEE Device Research Conference, for which is now a charter trustee. He served on the organizing committee of IEDM (1988–1992 and 1997–1999), having chaired both the solid-state device and detectors/sensors/displays committees. In 2005, he was named the William and Edna Macaleer Professor of Engineering and Applied Science. He also has been a symposium organizer for the Materials Research Society and on the SOS/SOI, EMC, and several other conference committees; he is the organizing chair for ISTDM 2006.

Journal  
of the SID